

High-speed bichromatic inspection of wheat kernels for mold and color class using high-power pulsed LEDs

Stephen R. Delwiche

Received: 21 November 2007 / Accepted: 21 January 2008 / Published online: 1 March 2008
© Springer Science+Business Media, LLC 2008

Abstract High-speed optical sorting of seeds in commercial processing is routinely practiced for removal of discolored seeds, seeds from volunteer plants, and non-seed objects. Sorters are conventionally based on monochromatic or bichromatic light from broad wavebands in the visible and near-infrared regions of energy. A particular challenge for these devices has been the recognition and removal of wheat kernels that have been damaged by the mold caused by the fungal disease Fusarium Head Blight. Previous research using an off-the-shelf bichromatic design on Fusarium-damaged wheat kernels demonstrated that approximately half of damaged kernels were positively detected. The research described herein examines an alternative design for bichromatic lighting and applies this design to two scenarios: sound vs. Fusarium-damaged wheat and red vs. white wheat. The new design utilizes two high-power (HP) LEDs and one silicon photo diode detector. The LEDs are flashed in alternating sequence at high frequency (2,000 Hz), such that during the half-cycle time period (0.25 ms) that each LED is on, reflected energy readings at a 10× sampling frequency are captured from a kernel in flight. This permits the capture of approximately 20 cycles of pulsed light during the time the free-falling kernel passes through the field of view of a fiber optic probe. A linear discriminant analysis (LDA) classification algorithm was applied that used two values derived from

the reflected energy readings. Based on the new design, the accuracy of sound vs. Fusarium-damaged classification was 78% on average; for red vs. white wheat classification, the average accuracy was 76%. Although these accuracy values are not at the level as that obtained from LDA models that utilize reflected energy readings at two wavelengths from stationary kernels (95% and 92% for sound vs. Fusarium-damaged and red vs. white, respectively), the new design offers an improvement over conventional bichromatic designs.

Keywords Fusarium Head Blight · Deoxynivalenol · DON · Bichromatic sorting · High-power · LED · Grain · Wheat

Introduction

In the United States, inspection of grain for official grade is conducted by the USDA Grain Inspection, Packers and Stockyards Administration. For wheat, inspection consists of the certification of wheat class (e.g., hard red winter, soft red winter, and six others) and grade (e.g., U.S. No. 1, U.S. No. 2, and four others). Among several factors that define grade, the level of damaged kernels greatly affects grade. Damage itself can occur by heat, frost, insect, pre-harvest sprouting, and, of primary interest in the current study, mold. One of the most prevalent forms of mold is called scab, which is caused by the fungus, *Fusarium graminearum*. Also known as Fusarium Head Blight (FHB), this disease is a worldwide problem that affects temperate climates where small grains (wheat, barley, corn, etc.) are grown. Often coincident with scab is the mycotoxin, deoxynivalenol (also called vomitoxin and DON), a metabolite of the mold. In the United States, DON is

Mention of trade names or commercial products is solely for the purpose of providing specific information and does not imply endorsement or recommendation by the USDA.

S. R. Delwiche (✉)
Food Safety Laboratory, USDA, Agricultural Research Service,
Beltsville Agricultural Research Center, Building 303,
BARC-East, Beltsville, Maryland 20705-2350, USA
e-mail: Stephen.Delwiche@ars.usda.gov

regulated by the FDA at an advisory level [1], such that the maximum recommended level is 1 mg/kg for finished wheat products for human consumption. Regulation elsewhere in the world, with more than 100 countries having established guidelines, can be even more stringent [2].

Fusarium Head Blight is not a newly discovered disease, as noted by its focus of study since the late 1800s [3]. However, in the past 20 years, coincident, though not fully proven, with the increased popularity of minimum tillage and corn in the crop rotation, FHB has become a recurring problem of the wheat growing regions of the US, with outbreaks occurring in the mid-1990s [4], and on through the current decade, such as in the soft red winter wheat growing areas of the eastern United States in 2003 and 2004. A conventional post-harvest method for reduction of DON is grain blending, in which the contaminant is diluted through combination with a cleaner lot. This practice could be banned in the United States should the FDA decide to change regulation from advisory level to action level status. Removal of Fusarium-damaged kernels can be accomplished at the various sequential stages of the wheat handling, such as by increasing the fan velocity of the combine to remove the generally lighter Fusarium-damaged kernels (at the risk of also losing sound kernels), and also at the mill through the use of either aspiration or density separation equipment [5, 6]. In the latter case, specific gravity tables, which rely on a difference in density of sound and Fusarium-damaged kernels, are very expensive, energy intensive, and limited in throughput. Hence, removal of Fusarium-damaged kernels by optical sorting technology is under consideration as an alternative to current mechanical practices.

Optical measurement techniques fall into two general categories, spectroscopy-based (visible or NIR) and image analysis-based. The first category, spectroscopy, was first examined by Dowell et al. [7]. In the second category, kernel morphology and color characteristics are the primary features used to distinguish damaged from healthy kernels [8, 9], with the *Fusarium* damage characterized by kernels having a white or pinkish color and being shriveled [10]. In the author's own studies [11–13], which involved visible and NIR spectroscopy on individual kernels, identification of Fusarium-damaged kernels of hard red winter wheat could be achieved at an accuracy of 95–97% with as few as two wavelengths. However, these studies were conducted under controlled laboratory conditions, in which each kernel was scanned at rest while placed in a machined trough on a black plate. Two analytical spectrometers were used, with one based on a 512-element silicon photodiode array (operating range of 380–879 nm) and the other based on a 128-element indium gallium arsenide array (1,000–1,700 nm usable range). From these studies, the best one or two wavelengths from each wavelength region (visible and

NIR) were determined from exhaustive searches of all possible wavelength combinations. The goal of wavelength selection was to use this information in the selection of filters (or other means of light dispersion) for bichromatic sorting devices. The restriction on the number of wavelengths not exceeding two was imposed in recognition of design specifications that require sorting devices to be very fast, which is achieved by a simple optical configuration.

In a later study by the author, in which a commercial sorter was used, commercial wheat samples of varying degrees of *Fusarium* damage were bichromatically sorted by utilizing a broad visible waveband (675 nm) and a broad NIR waveband (1,480 nm) [14]. With operating conditions set at a feed-rate of 0.33 kg/(min-channel) and a preset mass rejection rate of 10% for 43 samples ranging in DON concentration from low (<1.0 mg/kg) to very high (>20 mg/kg), approximately one-half of the Fusarium-damaged kernels were removed from one pass of sorting. This was in contrast to the >95% accuracy that was previously demonstrated as achievable under controlled laboratory, kernel-at-rest conditions. Therefore, the current study was designed to examine the gulf between the laboratory and high-speed environments, with the goal of developing new design criteria for high-speed (1–2 ms per kernel) sorting devices in order to reach the goal of 95% sorting accuracy.

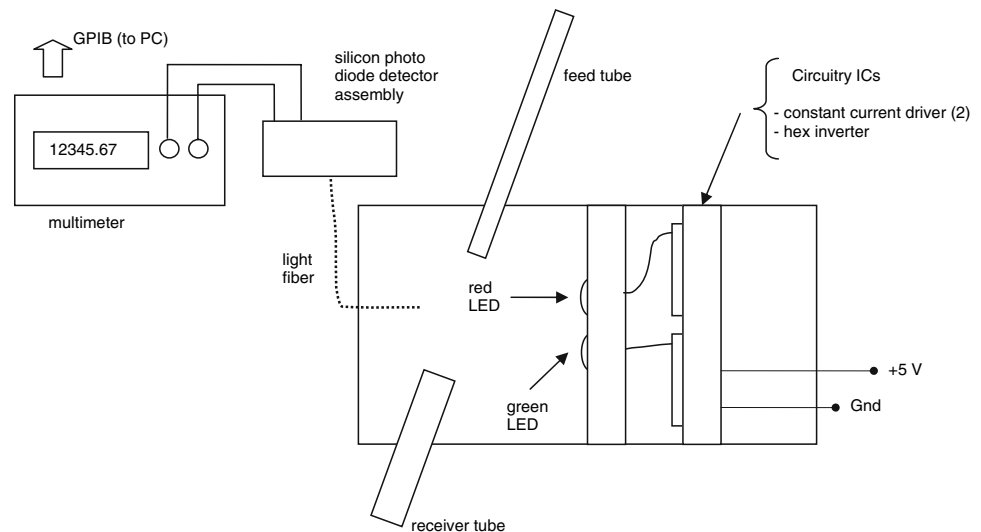
The objective of this study was to evaluate a pulsed LED-based illumination design for bichromatic optical sorting of free-falling cereal grains for detection of Fusarium-damage and for color classification. In addition to the new hardware design, two computed terms (the slope and coefficient of determination) that relate the reflected light response of one LED to a second LED are evaluated for their utility as input parameters to a classification algorithm that distinguishes sound and mold-damaged kernels. This system is also tested on distinguishing red wheat kernels from white wheat kernels.

Materials and methods

Equipment layout

A sketch of the apparatus for real-time inspection of free-falling kernels is shown in Fig. 1. This device consists of a stainless steel tube (914 mm length \times 6.3 mm ID) inclined at a 70° angle with respect to the horizontal. The inclination angle of the tube is slightly greater than that for an open channel of a commercial sorter because of the need to compensate for a large frictional force that occurs between the kernel and the tube's interior wall. The lower end of the tube terminates in a plastic electronics assembly box (120 mm width \times 64 mm height \times 40 mm depth) whose

Fig. 1 Schematic of high-speed single kernel inspection apparatus



two opposing faces are open. A short stub of 12-mm (1/2-inch) (OD) stainless steel tubing protrudes through the bottom of the assembly box and is used to receive the free-falling kernels. A distance of approximately 30 mm, as measured along a straight line path between the feed and receiver tubes, forms the region for kernel illumination and reflected energy capture by a fiber bundle. The terminal end of the multi-fiber bundle, with internal diameter of 5 mm, is oriented in a perpendicular direction to the trajectory path of the kernel. The opposite end of the fiber bundle is connected by SMA connector to a silicon detector/amplifier assembly (Hamamatsu, Model C6386-01, Hamamatsu City, Japan). The analog signal from this amplifier is digitized and stored by a multimeter (Hewlett Packard, Model 3458A). Digital data from the multimeter is transferred to a personal computer (PC) via a GPIB interface.

Illumination

A pair of pulse-width-modulated (PWM), high-power (~ 1 W) light emitting diodes (HP-LEDs) is used to illuminate the kernel in free-fall. As the kernel departs from the feed tube, it is subjected to alternating pulses of red and green light that are produced from the two HP-LEDs [Luxeon I Emitters LXHL-PM01 (green) and LXHL-PD01 (red), Phillips Lumileds Lighting Company, San Jose, CA]. The nominal peak wavelengths for the green and red LEDs are 530 and 627 nm, respectively. The full-width-at-half-maximum (FWHM) bandpasses of these LEDs (as specified by the manufacturer) are 35 and 20 nm, respectively. The peak wavelengths were selected from the seven commercially available color choices based on the author's previous research on wavelength pairings for detection of *Fusarium* damage [13].

Because the LEDs have a very short turn-on time (< 100 ns), it is possible to pulse these units at a frequency that is fast enough to allow the capture of many cycles of reflected energy readings during the time interval (~ 3 –6 ms) that a falling kernel passes through the field of view of the fiber optic probe. The actual frequency, set at 2,000 Hz, is limited by the controller board (PCI-6251, National Instruments, Austin, TX), such that approximately 20 cycles of readings are captured as the kernel traverses the probe's field of view. The two LEDs are flashed in sequence, with one LED turned on for one half-cycle while the other LED is off. During the second half cycle, the reverse occurs; the second LED is on while the first is off. The electronics design for the control of the LEDs is shown in Fig. 2. At the heart of the control circuitry is a 16-pin IC (MAXIM No. MAX6968, Dallas Semiconductor, Sunnyvale, CA) that is specifically designed to supply power to conventional LEDs, albeit at a lower current per channel

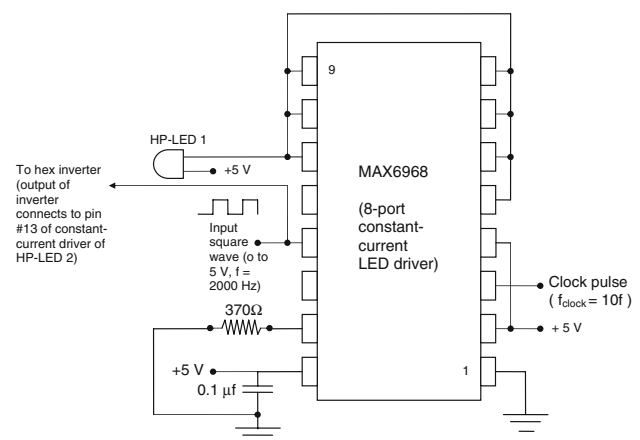


Fig. 2 Schematic of electronics design of high-power (HP) LED current supply circuit

(55 mA maximum) than that required for driving high-power LEDs (nominally 350 mA each). Seven output channels are tied together to supply the needed current. One current driver IC is used for each LED. A hex inverter, connected to the output-enable (\overline{OE}) pin of each driver, synchronizes the ICs to be exactly one-half cycle out of phase with respect to each other. Pulse control is performed in the Labview (v. 8.2) environment.

Samples

Two sets of wheat kernels were utilized. For the first set, breeders' advanced lines and commercial releases of *Fusarium*-inoculated soft red winter wheat were grown near Blacksburg, Virginia and harvested in summer 2005. Of more than 60 samples supplied, 20 were selected at random. From each sample, equal numbers of sound and *Fusarium*-damaged kernels were hand-selected based on human visual inspection. *Fusarium*-damaged kernels were identified from their faded, chalky appearance and shriveled texture. Altogether, a total of 24 healthy and 24 *Fusarium*-damaged kernels were selected from each sample.

The second set, consisting of commercial releases or breeders advanced lines of 10 red genotypes (FGIS57570, 'Waverly', 'Kulm', 'Sharpbristol', 'TAM 105', 'Len', 'Dodge', 'Seward', 'Nekota', and an unknown genotype from Berthoud, CO) and nine white genotypes [ID0604, 'Otis', 'Blanca Grande' (two independent samples), 'Nufontier', 'Klasic', 'Arlin', 'Snow White', 'Nuhorizon', and 'Rio Blanco'], was obtained from the USDA Grain Marketing and Production Research Center (Manhattan, KS). Harvest year and growing location were unavailable. From each sample, 30 kernels were selected at random.

Operation

A Visual Basic (version 6) program was written to send command instructions to the multimeter for capturing and transmitting reflected energy readings. Sampling rate (40,000/s) and number of sample points (1,000) were selected to capture sufficient data from the free-falling kernel while in the field of view of the fiber probe. The start of data capture was controlled by the multimeter's internal trigger. Reflected energy readings were eventually stored to external files in ASCII format, whereupon signal processing of the energy readings was performed at a later time. Because there was no synchronization between the LED cycles and the reflected energy readings during the time of data collection, the status of the LEDs with respect to the captured energy readings was ascertained from post-processing. The post-processing program was designed to search for the single greatest reflected energy reading and

assign this to a half-cycle in which the red LED was turned on (the red LED was more intense than the green LED). Having found the maximum reading, the two readings within the half-cycle that corresponded to the start and end points were subsequently identified. The interior eight readings were then averaged to form one reading per LED half-cycle. Likewise, all preceding and following half-cycles were processed in the same manner, thus producing a reduced ($1/10\times$) set of readings that alternated between red and green illumination responses. The subsequent classification analysis involved the pairing of green light to red light readings of adjoining half cycles. Because the time between adjoining processed reflected energy readings (i.e., the half-cycle time) was small (0.25 ms) with respect to the speed of the free-falling kernel (roughly 1 m/s), the assumption was made that the adjoining readings used to produce a pair of green- and red-light readings could be treated as one collective time interval.

Analysis

Upon initial processing, a total of 50 reflected energy readings under red light (627 nm, 20 nm FWHM) illumination and an equal number of readings under green light (530 nm, 35 nm FWHM) illumination were available, which represented a 25-ms time window. However, depending on the velocity and length of the kernel, the actual number of pairs of reduced readings in which the kernel was in the field of view of the fiber bundle probe was typically between 15 and 25. From this set of paired responses from each kernel, the green light responses were linearly regressed onto the red light responses. Two results from the regression analysis, the slope of the line of best fit and the corresponding coefficient of determination (r^2), were used as input parameters in a linear discriminant analysis (LDA) model for classifying a seed into one of two categories (i.e., sound vs. *Fusarium*-damaged, red vs. white). Comparable non-parametric classification models, such as *k*-nearest neighbor, did not reveal improved performance compared to LDA (results not shown). Consequently, all classification results reported herein were based on LDA. It was postulated that the slope, which encapsulates the relationship between the reflected energies under two wavelengths of visible light illumination would be sensitive to color variation between kernel classes, as caused by the differences in pigments within the seed coat. The coefficient of determination, on the other hand, was postulated to be sensitive to surface textural differences between kernel classes. Given these hypotheses, it was expected that the coefficient of determination would have a greater role in classification of sound and *Fusarium*-damaged wheat than in classification of red and white wheat because of the varied texture of *Fusarium*-damaged

kernels. Classification accuracy was reported as the percentages of kernels in each category correctly classified, based on a leave-one-out cross validation. Data reduction and classification analyses were performed in SAS (version 9), using the DISCRIM procedure for the LDA [15].

For the purpose of comparing the classification accuracy of the free-falling kernel apparatus with expectations (from previous studies) of accuracies that could be achieved under controlled laboratory, kernel-at-rest conditions, the kernels of each sample were also individually scanned at rest by a 512-element silicon photodiode array, as described in Delwiche [11]. A 250-ms integration time, with 10 successive scans per spectrum, was used for each kernel. Dark-current-adjusted, referenced (against a tile of polytetrafluoroethylene, i.e., 'spectralon') energy readings were stored as $\log(1/R)$.

The data from the diode array spectrometer were also processed in SAS. Spectral data were first transformed back to reflectance, whereupon a Gaussian waveform of 20 nm (FWHM) was convolved onto each spectrum for the purpose of mimicking the illumination conditions of the free-falling kernel setup. From this convolved spectrum, the reflectance value centered at 627 nm ($R_{627\text{ nm}}$) was selected. This procedure was repeated, using a Gaussian waveform of 35 nm for convolution, in order to select a reflectance value centered at 530 nm ($R_{530\text{ nm}}$). Classification by LDA was subsequently performed using these two reflectance values as input parameters.

Results

Typical time-of-flight responses of two free-falling Fusarium-damaged kernels from one sample are depicted in Fig. 3. These two kernels were purposely selected to demonstrate the large kernel-to-kernel variation in captured reflected energy. Not only are the peak levels of energy different between the two kernels, but the shapes of time-domain traces are also different, with the kernel in the upper graph (A) demonstrating a symmetrical shape under both red and green illumination, compared to the kernel's trace in the lower graph (B) having much less symmetry, though still possessing some degree of correlation between red and green responses. Similar overall curve shapes were observed for the sound kernels of this set and also for the kernels of the red and white wheat set, such that sample traces of these kernels are not shown.

A scatter plot of the two free-falling classification parameters (slope and r^2) of all sound and Fusarium-damaged kernels ($n = 480$ kernels, each) is shown in Fig. 4. Apparent from this plot is the fact that while a general separation exists between the two categories, there is also a certain degree of overlap. Based on these two

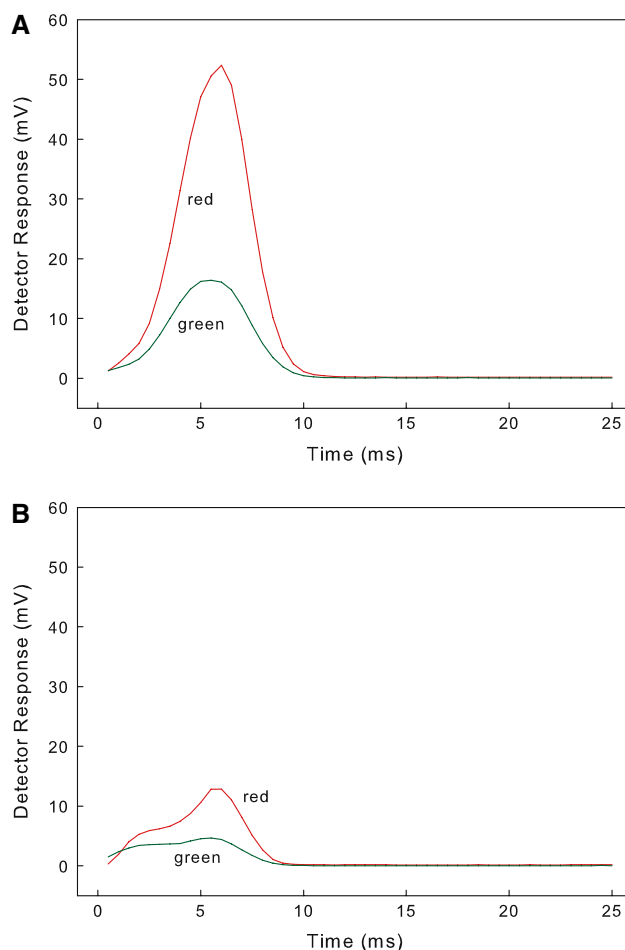


Fig. 3 Examples of reflected energy responses of two free-falling Fusarium-damaged wheat kernels subjected to red (peak = 627 nm) and green (peak = 530 nm) light

parameters, the LDA cross-validation accuracies were 83% and 72% for sound and Fusarium-damaged categories, respectively, yielding an average accuracy of 78% (Table 1). Of the two parameters, the slope, with an average classification accuracy of 75%, was a much better one-term discriminator than the coefficient of determination, which produced an average accuracy of 56%. Thus, color, rather than texture as sensed by the free-falling apparatus, was the dominant classifier. To gauge the margin for improvement if the free-falling system were to be refined, the classification accuracies arising from LDA using the reflectances at two wavelengths ($R_{530\text{ nm}}$, $R_{627\text{ nm}}$) when the kernel was at rest are also listed in Table 1. These accuracies, averaging 95% when both wavelengths are used, were on par with the author's earlier published results [13]. A scatter plot of the stationary-kernel reflectance at two wavelengths is shown in Fig. 5. This plot shows a more distinct separation of the two categories than the free-falling plot of Fig. 4.

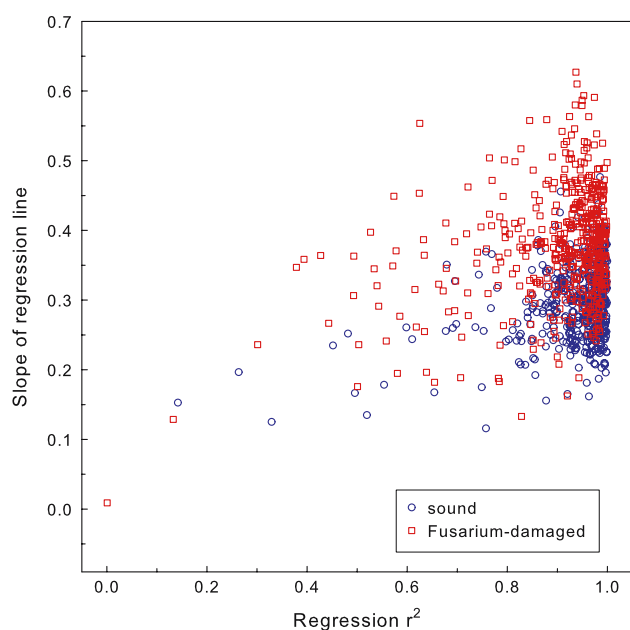


Fig. 4 Plot of classification parameters (slope, r^2) from the free-falling apparatus of sound and Fusarium-damaged wheat kernels, consisting of 20 varieties or lines of soft red winter wheat from which 24 Fusarium-damaged and 24 normal kernels per variety/line were selected at random

Table 1 Summary of accuracies of linear discriminant analysis (LDA) models for classification of sound and Fusarium-damaged wheat kernels

State of Kernel	Parameters used in LDA model	Percentage of correctly classified kernels by LDA cross-validation		
		Sound	Fusarium-damaged	Average
Free-falling	Slope, S	79.4	71.2	75.3
	Coefficient of determination, r^2	76.5	35.6	56.0
	S , r^2	82.7	72.5	77.6
Stationary	$R_{530 \text{ nm}}$	77.1	65.8	71.5
	$R_{627 \text{ nm}}$	60.2	55.2	57.7
	$R_{530 \text{ nm}}$, $R_{627 \text{ nm}}$	95.6	94.8	95.2

Similar to the scatter plot of Fig. 4, the plot contained in Fig. 6 shows that the two free-falling classification parameters for red and white wheat provided a certain degree of separation of the color classes; however, this separation was not perfect. A scatter plot of the at-rest reflectances of these same kernels is shown in Fig. 7, along with a summary of the LDA classification results listed in Table 2. Apparent from the scatter plots, and confirmed by the tabulated accuracies, red and white kernels were more difficult to distinguish than sound and Fusarium-damaged kernels. The classification accuracy from the free-falling

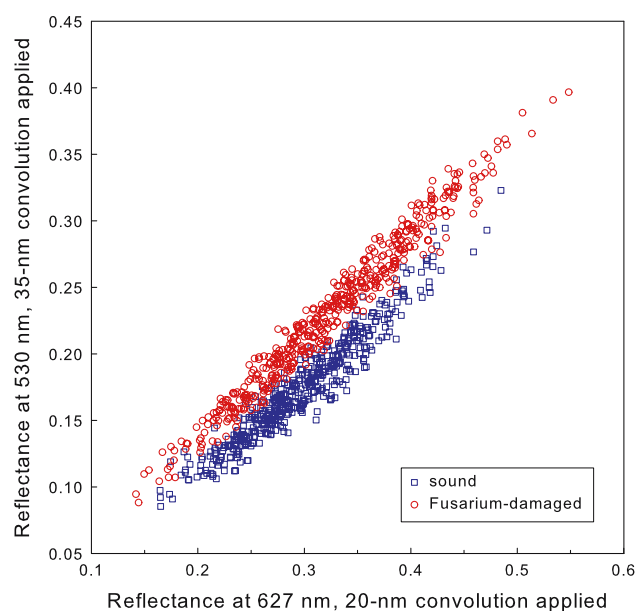


Fig. 5 Plot of classification parameters from stationary, diode array apparatus for the same kernels described in Fig. 4. The classification parameters are reflectance values at 530 and 627 nm

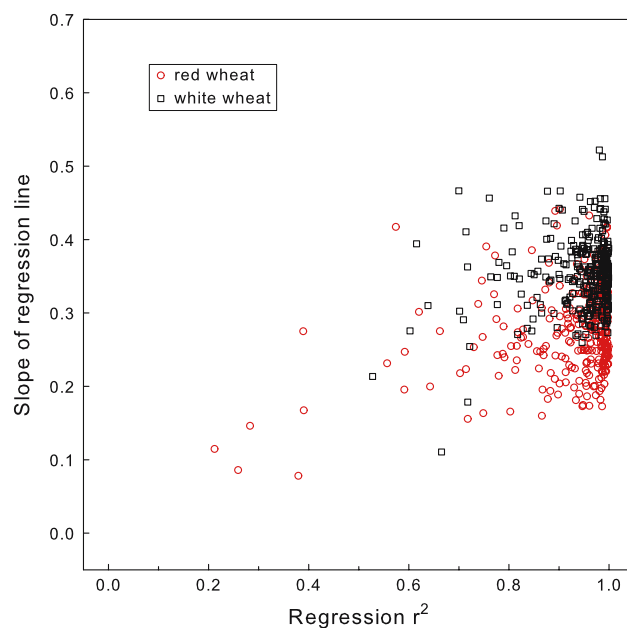


Fig. 6 Plot of classification parameters (slope, r^2) from the free-falling apparatus of red and white wheat kernels, consisting of 10 varieties or lines of red wheat and 10 varieties or lines of white wheat from which 30 kernels per variety/line were randomly selected. The classification parameters are the slope of the linear regression equation and coefficient of determination arising from the regression of the green light response onto the red light response

system averaged 76% for the red vs. white set, compared to 78% for the sound vs. Fusarium-damaged set. Consistent with this ranking, the stationary system accuracy was also lower for the red vs. white (92%) than for the sound vs.

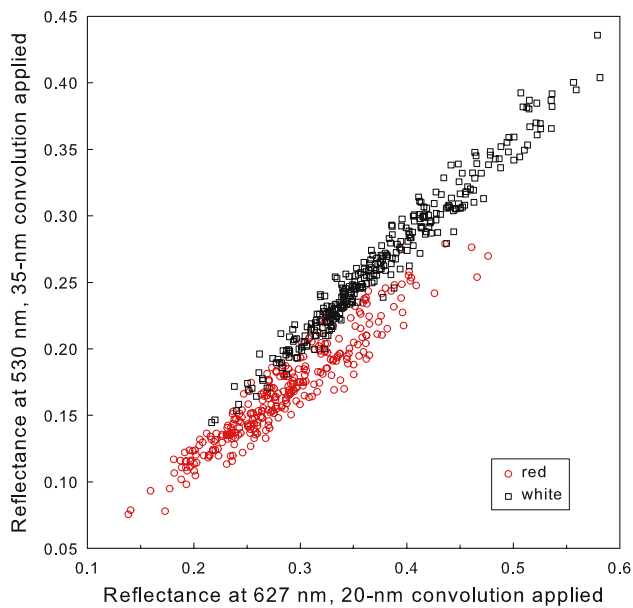


Fig. 7 Plot of classification parameters from the stationary, diode array apparatus for the same kernels described in Fig. 6. The classification parameters are reflectance values at 530 and 627 nm

Table 2 Summary of accuracies of linear discriminant analysis (LDA) models for classification of red and white wheat kernels

State of kernel	Parameters used in LDA model	Percentage of correctly classified kernels by LDA cross-validation		
		Red	White	Average
Free-falling	Slope, S	75.0	76.7	75.8
	Coefficient of determination, r^2	31.0	75.0	53.0
	S , r^2	74.7	77.7	76.2
Stationary	$R_{530 \text{ nm}}$	86.7	80.0	83.3
	$R_{627 \text{ nm}}$	78.0	71.7	74.8
	$R_{530 \text{ nm}}$, $R_{627 \text{ nm}}$	92.3	92.7	92.5

Fusarium-damaged set (95%). As with the other two sets of data, the slope of the regression equation was the more useful parameter in the classification model, such that, by itself, slope yielded an average classification accuracy of 76%. In fact, at an average accuracy of 53%, the coefficient of determination parameter was only marginally better than chance alone.

Discussion

From the results of the current study, the ability to correctly discriminate free-falling wheat kernels (sound from Fusarium-damaged or red from white) is lower than when the

kernels are stationary. These results are in general agreement with the author's previous studies that demonstrated a 95% accuracy of correctly identifying Fusarium-damaged kernels at rest, using two wavelengths [13], and a corresponding 50% accuracy for high-speed bichromatic sorting [14]. Encouragingly, the present research demonstrates an improvement in damaged kernel detection, with more than 70% of the Fusarium-damaged kernels in free-fall correctly identified. The aim of ongoing research is to enact changes to either lighting or probe placement in order to improve the accuracy to 95% or better. Considering that the literature documents cases of 99% accuracy for red vs. white wheat kernel identification by visible/NIR spectroscopy (albeit with reliance on spectral readings from a broad near infrared wavelength region, reduced in mathematical dimension by partial least squares analysis) [16], there appears to be the likely possibility of reaching similar levels of accuracy through design modifications of the free-falling system.

Based on the author's research of the past several years on the feasibility of utilizing high-speed optical sorting technologies (conventional and the author's unique design), the following insights are noted: (1) An accuracy of 95% or better can be achieved for recognition of Fusarium-damaged individual wheat kernels through the implementation of reflectance readings at two wavelengths of visible light (530 and 627 nm). However, at present, these accuracies are reached only under controlled laboratory conditions in which the kernel is at rest, rather than in free-fall. (2) Conventional high-speed optical bichromatic sorting under free-fall conditions results in the correct identification and removal of approximately one-half of the Fusarium-damaged kernels. (3) With a newly devised lighting, electronic, and data processing design for identifying Fusarium-damaged kernels in free-fall, an accuracy level of 72% has been reached. Research to improve this level to approach that of the stationary condition is currently ongoing.

Acknowledgments Dallas Semiconductor (Sunnyvale, CA) donated the current driver integrated circuits. The Fusarium-damaged wheat samples were supplied by Professor C. Griffey, Department of Crop and Soil Environmental Sciences, Virginia Polytechnic Institute and State University, Blacksburg, VA. The red and white wheat samples were provided by Dr Floyd Dowell, USDA Grain Marketing and Production Research Center, Manhattan, KS.

References

1. US Food and Drug Administration, Letter from Ronald Chesmore to State Agricultural Directors, State Feed Control Officials, and Food, Feed and Grain Trade Organizations on Advisory Levels for DON (vomitoxin) in Food and Feed (US Department of Health and Human Services, Public Health Service, Rockville, MD, September 16, 1993)

2. FAO, Worldwide regulations for mycotoxins in food and feed in 2003. Food and Nutrition Paper 81 (Food and Agriculture Organization of the United Nations, Rome, Italy, 2004)
3. R.W. Stack, in *Fusarium Head Blight of Wheat and Barley*, ed. by K.J. Leonard and W.R. Bushnell (American Phytopathological Society, St. Paul, MN, 2003), pp 1–34
4. L.P. Hart, *Plant Dis.* **82**, 625 (1998)
5. L.M. Seitz, W.D. Eustace, H.E. Mohr, M.D. Shogren, W.T. Yamazaki, *Cereal Chem.* **63**, 146 (1986)
6. R. Tkachuk, J.E. Dexter, K.H. Tipples, T.W. Nowicki, *Cereal Chem.* **68**, 428 (1991)
7. F.E. Dowell, M.S. Ram, L.M. Seitz, *Cereal Chem.* **76**, 573 (1999)
8. X. Luo, D.S. Jayas, S.J. Symons, *J. Cereal Sci.* **30**, 49 (1999)
9. R. Ruan, S. Ning, A. Song, A. Ning, R. Jones, P. Chen, *Cereal Chem.* **75**, 455 (1998)
10. D. Atanasoff, *J. Agr. Res.* **20**, 1 (1920)
11. S.R. Delwiche, *Trans. ASAE* **46**, 731 (2003)
12. S.R. Delwiche, G.A. Hareland, *Cereal Chem.* **81**, 643 (2004)
13. S.R. Delwiche, C.S. Gaines, *Appl. Eng. Agric.* **21**, 681 (2005)
14. S.R. Delwiche, T.C. Pearson, D.L. Brabec, *Plant Dis.* **89**, 1214 (2005)
15. SAS, *Proc Discrim. in Statistics Guide* (SAS Institute, Cary, NC, 1988)
16. F.E. Dowell, *Cereal Chem.* **75**, 142 (1998)